Integration of Biomechanical Parameters in Tetrahedral Mass-Spring Models for Virtual Surgery Simulation

Alessandro Sala, Giuseppe Turini, Mauro Ferrari, Franco Mosca, and Vincenzo Ferrari

Abstract— Surgical simulation requires to have an operating scenario as similar as possible to the real conditions that the surgeon is going to face. Not only visual and geometric patient properties are needed to be reproduced, but also physical and biomechanical properties are theoretically required.

In this paper a physically based patient specific simulator for solid organs is described, recalling the underlying theory and providing simulation results and comparisons.

The main biomechanical parameters (Young's modulus and density) have been integrated in a Mass-Spring-Damper model (MSDm) based on a tetrahedral structured network. The proposed algorithms allow the automatic setting of node mass and spring stiffness, while the damping coefficient have been modeled using the Rayleigh approach.

Moreover, the method automatically detects the organ external layer, allowing the usage of both the surface and internal Young's moduli: for the capsule (or stroma) and for the internal part (or parenchyma). Finally the model can be manually tuned to represent lesions with specific biomechanical properties.

The method has beed tested with various material samples. The results have shown a good visual realism ensuring the performance required by an interactive simulation.

I. INTRODUCTION

The need to train young surgeons both increasing their skills in performing practises and preserving patients security, encouraged the development of virtual simulators hopefully able to give realistic haptic and visual feedback.

A surgical simulator is a software application that takes inputs from surgical tool's shaped virtual interfaces and, running a physics engine on a virtual model, returns on screen a visual scenario of the deformed organs and optionally a haptic force feedback related to the user interactions.

A physics engine is a coded set of physical laws and methods (i.e.: gravity and Hooke's law) that applies on a virtual model to confer a realistic behaviour. This model of the organ is not just a 3D surface mesh, it is a physical representation in which geometry and topology of the primitive elements (i.e.: nodes and links) combined with physical and mechanical properties (i.e.: mass, stiffness) reproduce as faithfully as possible the shape and behaviour of the reference target (Fig. 1).
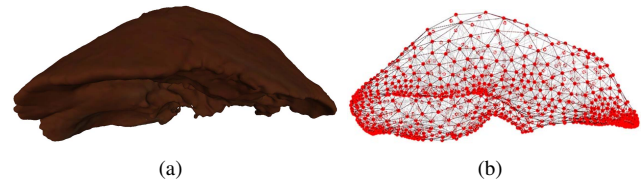

(a)   (b)

Fig. 1. Virtual models of a human liver: *(a)* shows the surface 3D model extracted from a medical dataset while *(b)* displays an example of a dense spring network model for real time biomechanical simulation.

In the last years two popular kinds of physical models has been proposed: Mass Spring Damper models (hereafter MSDm) and Finite Element Models (FEM).

FEM models lie in applying finite elements numerical techniques on geometrically simple shapes (e.g.: cubes, tetrahedra, exahedra etc.) involve physics engines based on difference equations of continuum mechanics theory; they are very realistic, particularly in their nonlinear formulation, but their computational requirements make themselves tough to be applied for real time virtual simulation [5].

On the contrary, MSDm are computationally inexpensive, but there is not a straightforward connection with material mechanics. Moreover, often the computation of the exact displacement is not required, but it is enough a plausible behaviour of the tissue's movement. Since the formulas that rule these models are trivial, the most challenging issue is to define a method to map the material properties into the MSDm coefficients [6].

Regarding MSDm geometry and topology, some efforts have been spent on cubic elements [19][1] but tetrahedral filling is by far the most popular meshing technique [6][16], as long as it is easily scalable and able to provide a good surface modelling limiting the number of elements [15].

One of the most prolific [24][16][12][19] works using triangular based shapes is given by Van Gelder [23]: in this work it is explained how to map biomechanical parameters into spring coefficients for 2D membranes, and a heuristical extension to tetrahedra is also provided. Few years later Lloyd [12] extended this work for tetrahedral meshes, proposing a theoretical derivation obtained minimizing the squared difference between FEM and springs network stiffness matrix's elements.

The purpose of our work is the integration of biomechanical parameters in MSDm physics models in order to enhance the accuracy of the simulation for interactive virtual surgery.

The virtual deformable model used in this paper is based on a MSDm with a tetrahedral structure; its vertices are called *nodes*, on which *masses* are applied, and its edges are called *links*, on which linear *springs* are applied.

During the simulation loop the physics engine computes the forces to be applied on all the nodes. These forces are generated both by internal springs and by external sources (user interactions, gravity etc.). Then, using the *Explicit Euler Integration*, accelerations and velocities can be computed and used to determine the next positions and velocities of the nodes. Finally, once updated the deformable model, the simulation loop can be reiterated.

II. PARAMETERS IDENTIFICATION

If we consider a MSDm defined by n nodes, at each timestep of the simulation loop we can define the displacement vector $\mathbf{u}^\top = [\mathbf{u}_1^\top, \ldots, \mathbf{u}_n^\top]$ where $\mathbf{u}_i^\top = [u_{ix}, u_{iy}, u_{iz}]$ is the displacement of the node i at the current timestep in respect of its initial position.

Therefore, we can derive the force induced by the displacement vector $\mathbf{u}$ applying the first cardinal equation of dynamics:

$$M\ddot{\mathbf{u}} = D\dot{\mathbf{u}} + K\mathbf{u} + \mathbf{f}_{\text{ext}} \qquad (1)$$

where M, D, K are $3n \times 3n$ square matrices respectively defining mass, damping and stiffness coefficients; $\mathbf{f}_{\text{ext}}$ is a $3n$ column vector, defining external forces applied to the nodes.

During each iteration, for each node i of the physics model, its velocity $\dot{\mathbf{u}}_i$ and displacement $\mathbf{u}_i$ are known from the previous integration phase; so, the three contributions of forces (damping, elastic, and external) in (1) can be computed and summed. Then, it is possible to proceed with the *Explicit Euler Integration* phase: obtaining the node acceleration $\ddot{\mathbf{u}}_i$ dividing this sum by the node mass m_i (see II-A). The resulting node acceleration will be used in the next iteration to compute both velocity and displacement of the node.

The virtual model is fully defined by its masses, springs, and dampers coefficients: therefore a biomechanical characterization needs arise from the identification of these properties by analyzing the target dense organ to be represented.

A. Nodes Mass Parametrization

The identification of the mass matrix M elements in (1) is not immediately related to the masses applied to nodes. In its most general formulation is positive definite, squared, and dense as it comes from the hessian of kinetic energy expressed using shape functions [7]. The off-diagonal terms help to preserve the linear and angular momentum and give inertial contributes not depending on the considered node.

A widely used approach (*mass lumping*) is to consider only the diagonal terms, corresponding to the 3D components of each node [6]. Lumping allows a intuitive physical association: applying a mass to each node. For the single node, the three mass components were considered equals (i.e.: the inertial contribute is the same in all directions); so in this

case the node mass m_i to be determined is a simple scalar value.

If the material density ρ is known, the node mass m_i can be computed considering the node i surrounding volume, so the problem rephrase in defining a volumetric region belonging to each node. Barycentric and Voronoi volume splitting are two common procedures to establish this association; they divide the volume in a different way but both are based on the idea of giving a volumetric contribution to each node considering the volume defined by the set of incident tetrahedra on that node. Hence, the node mass m_i derives from the sum of the mass contributions calculated for each tetrahedron incident on the node i.

1) The barycentric mass-lumping: The barycentric subdivision scheme [24][16] splits each tetrahedron into four isovolumes defined by the midlines, each referring to one of its nodes; this, considering the density uniform, means to assign the same mass contribute to each node of the tetrahedron. Obviously the lumped tetrahedron preserve, at least in its undeformed configuration, the same barycentre of the dense one.

$$m_i = \frac{1}{4} \sum_{t \in \Omega_i} \rho_t \, V(t) \qquad (2)$$

In (2) Ω_i is the set of tetrahedra sharing the node i (Fig. 2(c)), while ρ_t and $V(t)$ are respectively the density and volume of the tetrahedron t.

2) The Voronoi mass-lumping: Another very intuitive approach is to associate each point in the space to the nearest node, which means to determine the Voronoi tessellation of the model volume using its nodes as the input set of points. Given a set Ψ of nodes, the Voronoi division confers to each node i a subdomain (volume cell) $C(i, \Psi)$ whose points q are nearer to i than to all the other nodes, and defined by:

$$C(i, \Psi) = \{q \in \mathbb{R}^3 : L(q, i) < L(q, j), \forall j \in \Psi - \{i\}\} \quad (3)$$

where $L(q, i)$ represents the distance between the point q and the position of the node i. Hence, the Voronoi diagram defined in (3) can be easily computed for a tetrahedral model redefining the cell:

$$C(i, \Psi) = \bigcup_{t \in \Omega_i} C(i, \Psi_t) \qquad (4)$$

where Ψ_t represents the set of nodes of the tetrahedron t.

In (4) the Voronoi cell $C(i, \Psi)$ of the node i is defined as the union of the cells, associated to the node i, computed tessellating all the tetrahedra in Ω_i (that are the tetrahedra sharing the node i). Therefore, we can assign the appropriate mass m_i to each node i simply multiplying the volume of its Voronoi cell $C(i, \Psi)$ by the material density ρ:

$$m_i = \sum_{t \in \Omega_i} \rho_t \, V(C(i, \Psi_t)) \qquad (5)$$

where $C(i, \Psi_t)$ is the cell associated to the node i and related to the Voronoi tesselation of the tetrahedron t.

| Aspect Ratio	1.0	0.6	0.2
$(V_{\min}^{\mathrm{VOR}} - V^{\mathrm{BAR}}) \,/\, V^{\mathrm{BAR}}$	$-0,00\%$	$-50,74\%$	$-74,50\%$
$(V_{\max}^{\mathrm{VOR}} - V^{\mathrm{BAR}}) \,/\, V^{\mathrm{BAR}}$	$+0,00\%$	$+152,23\%$	$+223,48\%$

Fig. 2. The cube model and its mass-spring network respectively in *(a)* and *(b)*: *(c)* highlights (in bright red) the tetrahedra shared by the red node-vertex in *(b)*, while *(d)* shows the tetrahedra (in bright blue) incident on the blue spring-edge in *(b)*.

Table I shows a comparison between the barycentric and Voronoi mass lumping techniques applied on the 4 nodes of sample tetrahedra with different values of aspect ratio (AR): in this case defined as the min solid angle of the tetrahedron divided by the min solid angle of the regular tetrahedron. Varying the tetrahedron shape, starting from a regular tetrahedron and reducing its AR, an increasing divergence of the Voronoi cell volume in respect to the barycentric cell volume is highlighted. The comparison is given as the percentage difference between the Voronoi cells with min ($V_{\min}^{\mathrm{VOR}}$) and max ($V_{\max}^{\mathrm{VOR}}$) volume with respect to the barycentric cell volume (V^{BAR}).

The barycentric mass lumping takes into account only the tetrahedron volume, whereas the Voronoi strategy considers also its shape. Both techniques have been implemented, so the appropriate method can be chosen case by case.

B. Springs Stiffness Parametrization

The modelling of spring stiffness in the description of biological soft tissues requires a strong idealization: in most cases, biological tissues have non linear, non homogeneous, anisotropic, viscoelastic properties. Only considering linear elastic homogeneous isotropic materials' laws the tissue behaviour can be associated to the Hooke's spring law. This states that the force generated by the spring connecting node i and node j can be approximated by $\mathbf{f}_{ij} = -k_{ij} \cdot \mathbf{v}_{ij}$; where $\mathbf{v}_{ij}$ is the displacement of the spring's end from its equilibrium position, $\mathbf{f}_{ij}$ is the elastic force exerted by the spring, and k_{ij} is the constant spring stiffness coefficient.

It is clear that the stiffness coefficient k_{ij} of the spring connecting node i and node j, should be mapped by the stiffness tensor C that correlates strains ε and stresses σ in $\sigma = C \cdot \varepsilon$; if only the principal directions are considered, this relation reduces to $\sigma = E \cdot \varepsilon$ where E is the Young's modulus, easily recoverable in literature.

Conceptually the spring stiffness should be proportional both to the Young's modulus and to the tetrahedron edge length, and should map the stiffness of the material volume surrounding the spring. Based on these concepts, we applied Lloyd's approach [12], that is an extention of the work of Van Gelder to tetrahedral elements. The proposed method compares a stiffness matrix derived from FEM formulation with a springs network derived one, obtaining the formula

$$k_{ij} = \sum_{t \in \Omega_{ij}} \frac{2\sqrt{2}}{25} \, l_t \, E \qquad (6)$$
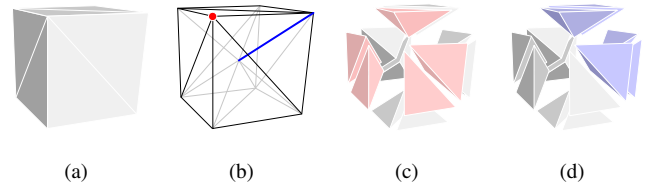
where the spring coefficient connecting the vertices i and j is computed considering the set Ω_{ij} of tetrahedra sharing the ij edge (Fig. 2(d)). Instead of simply considering the edge length l_{ij}, it is considered the fictitious length $l_t = (V(t)(12/\sqrt{2}))^{\frac{1}{3}}$: computed as the edge length of a regular tetrahedron with the same volume $V(t)$ of the tetrahedron t, as explained in [12].

Furthermore, dense organs are basically composed by an internal section (that is the functional part, or parenchyma), and an external capsule (namely the supportive framework, or stroma). These two parts have specific biomechanical properties, so being able to properly model each of them is crucial [9]. Hence, we have decoupled the modeling of the surface layer from the internal network of the MSDm (Fig. 5(a)), allowing the automatic detection of the capsule (and the parenchyma) and enabling the use of different Young's moduli. Moreover, the virtual model can be manually configured to represent specific lesions with different biomechanical properties in respect to the healthy tissue.

C. Dampers Coefficients Parametrization

Damping confers realism and stability to mechanical systems. One of the most used [10] and straightforward method in the determination of damping matrix D in (1) is the Rayleigh formula [11]; this, in its simplest formulation $D = \alpha \, M + \beta \, K$, considers D as the sum of two different weighted contributions: an inertial term proportional to the mass whereas the second term is proportional to the stiffness and tends to reduce the oscillations of the springs network [21].

Even if some methods to calculate the two Rayleigh parameters α and β have been proposed [2], very often a modal analysis of the considered system is not feasible due to the difficulties to properly test the organ damping parameters; furthermore the interactions involved in a virtual surgical procedure simulation do not require an accurate damping tuning to obtain a realistic behaviour of the virtual anatomy.

For these reasons, it's common practice to empirically tune these parameters to visually fit the tissue behaviour.

III. IMPLEMENTATION

Our implementation relies on a custom MSDm, that is an extension of that available from the CHAI 3D [4]. As already stated, the structure of the deformable model is based on a tetrahedral mesh, representing the volume of the target organ. This was generated through a pipeline that takes in input
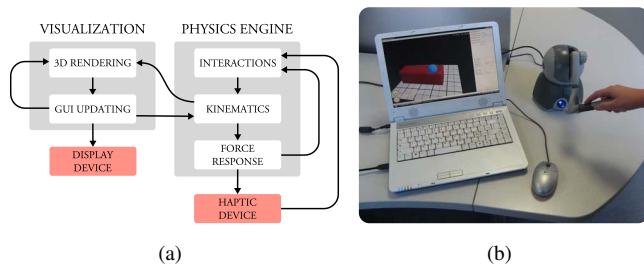
(a)   (b)

Fig. 3.   The simulation system: on the left the logical diagram of the simulator and on the right a photo during a test case.
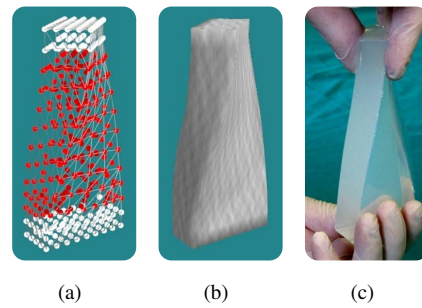

(a)   (b)   (c)

Fig. 4.   Visual comparison between the virtual model, both in *wireframe (a)* and *texturized (b)* version, and the *real (c)* agarose phantom.

a medical dataset (CT or MRI), generates a surface mesh using segmentation techniques (Fig. 1(a)) and then, after an optimization phase, creates the final volumetric representation as a tetrahedral mesh (Fig. 1(b)). This process requires the usage of various software: a custom pipeline based on ITK-SNAP [8] for the dataset segmentation, MeshLab [3] to clean and optimize the surface model, NETGEN [20] for the generation of the tetrahedral mesh and Autodesk® Maya® for the texturing. Finally the resulting structure is stored in our custom MSDm.

Once the network is defined, the tuning of nodes and springs has to be applied; to do this we have extended the MSDm adding edge-vertex and edge-tetrahedron topologies. The mass lumping has been implemented replacing the standard barycentric approach with a Voronoi based technique realized using Voro++ library [18] to compute the Voronoi tessellation of the tetrahedra, as shown in (3) and (4). Similarly, the springs properties have been evaluated exploiting the edge-tetrahedron topology to determine the volumes required to solve (6). At last the Rayleigh damping coefficients α and β have been compressed in a single inertial term applied to each node. Although this method requires to extend again the MSDm with edge-vertex topology, it improves the performance of the simulation.

The complete software simulation system is a multi-threaded application providing visual and tactile feedback. The graphic rendering is carried out using the CHAI 3D scene graph for the virtual environment and the Nokia® Qt® library for the user interface; while a secondary thread elaborates the dynamics, collision detection and force response relying on the CHAI 3D funcionalities (Fig. 3(a)).

IV. RESULTS

In order to test the realism and physical plausibility of the virtual simulation, it was decided to perform some visual comparison tests between the virtual MSDm and real material samples.

A. Test A: Agarose Sample

The first experiment was performed to evaluate the realism of a global deformation: in this case a torque. We decided to use a real agarose sample shaped in a rectangular prism ($2\,\text{cm} \times 5\,\text{cm} \times 10\,\text{cm}$, see Fig. 4(c)), and with similar mechanical parameters typical of a in vivo human liver; while the virtual

model was composed by approximately 400 nodes and 1400 tetrahedra (Fig. 4(a)).

Agarose is a linear polymer showing mechanical and viscous characteristics similar to those of soft tissues, and then it is considered a good substitute of real specimen, often difficult to recover. In addition Luo et al. [13] demonstrated that subsists a linear relationship between the percentual concentration of agarose and the Young's Modulus in the range 1-5%, so the mechanical parameters can be easily estimated. As Nava et al. [17] estimated Young's Modulus for an in vivo human liver as $20\,\text{kPa}$ ca., so the regression line in [13] was used to obtain the right concentration to reach this stiffness, and this was found to be 2,64%.

Once mixed, the composite was warmed at $150\,^\circ\text{C}$ ca. for about 45 minutes to reach a homogeneous solubility; it was then poured into the mold and let rest until get back cold and solid. Finally a torsion of both the virtual model and the specimen is applied, fixing the top and bottom borders of the virtual model to emulate the constraints imposed by the user hands on the real agarose phantom (Fig. 4).

B. Test B: Bovine Liver Sample

The second test was carried out to visually examine a local deformation: as the pressure of a finger on a biological tissue. This time, we have decided to compare the virtual model with a sample of a bovine liver.

The organ has been dissected in a rectangular prism ($10\,\text{cm} \times 10\,\text{cm} \times 30\,\text{cm}$), having part of the stroma on the upper side (Fig. 5(c)). In this way, we have been able to test the capsule-parenchyma modeling using a MSDm composed by about 640 nodes and about 2600 tetrahedra (Fig. 5(a)).

The biomechanical properties of the bovine liver tissue have been widely investigated in literature. Accordingly with the studies of Shan et al. [22] and Hollenstein et al. [9], we have chosen a Young's Modulus of $20\,\text{kPa}$ for the parenchyma and $60\,\text{kPa}$ for the stroma.

Lastly, we have applied a localized pressure on the virtual and real samples. The visual comparison illustrated in (Fig. 5) shows the realism of the deformation simulated, highlighting the lack of a significant global deformation component as it happens in the real scenario.

All the tests were performed on a consumer notebook: Intel Core 2 Duo 2.60 GHz CPU with 4Gb RAM running
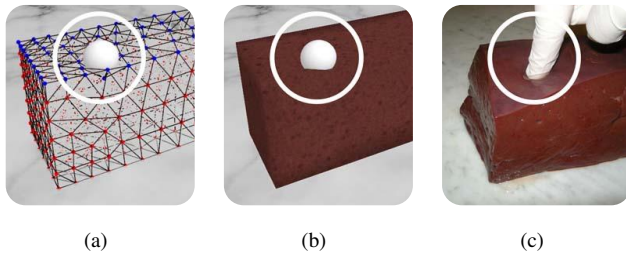
Fig. 5. Visual comparison of a local deformation (white circle) between the virtual model *(b)* and the real sample *(c)* of a bovine liver; image *(a)* shows the structure of the MSDm, highlighting the stroma (blue) and the parenchyma (red).

a 32bit Microsoft® Windows Vista®; using a Sensable® Phantom Omni® device for the haptic feedback (Fig. 3(b)). During the tests, the mesh loading (including the biomechanical parametrization of the MSDm) required only few seconds whereas the graphic rendering was performed with a frame rate of about 50 fps and the physic engine update rate was stably over 1k iterations per second.

V. CONCLUSIONS AND FUTURE WORKS

This article presents a virtual model based on a parametrization of biomechanical properties of dense human organs. The model consists in a Mass-Spring-Damper model with a tetrahedral structured network, in which nodes are characterized by masses and damping coefficients, while links (connecting node pairs) are described by spring stiffness constants. These settings are retrieved from biomechanical parameters (tissue density, internal and surface Young's Moduli), that can be obtained from literature, or from *ex vivo* testing; while the network structure is derived from a tetrahedral model of the organ.

Our formulation has proven to be a good tradeoff between an accurate physical description and the performance required for an interactive simulation.

This approach will be applied for robotics surgery simulation of the whole abdominal district [14].

VI. ACKNOWLEDGMENT

REFERENCES

[1] Vincent Baudet, Michael Beuve, Fabrice Jaillet, behzad Shariat, and Florence Zara. Integrating tensile parameters in 3d mass-spring system. Technical Report RR-LIRIS-2007-004, LIRIS, Universit Lyon 1, feb 2007.

[2] Indrajit Chowdhury and Dasgupta Shambhu P. Computation of rayleigh damping coefficients for large systems. Technical report, Department of Civil Engineering, Indian Institute of Technology, 1998.

[3] Paolo Cignoni, Massimiliano Corsini, and Guido Ranzuglia. Meshlab: an open-source 3d mesh processing system. *ERCIM News*, 73:45–46, apr 2008.

[4] F. Conti, F. Barbagli, R. Balaniuk, M. Halg, C. Lu, D. Morris, L. Sentis, E. Vileshin, J. Warren, O. Khatib, and J. K. Salisbury. The CHAI libraries. In *Proc. of EuroHaptics*, pages 496–500, Dublin, Irland, jul 2003.

[5] Stéphane Cotin, Hervé Delingette, and Nicholas Ayache. Real-time elastic deformations of soft tissues for surgery simulation. *IEEE Transactions on Visualization and Computer Graphics*, 5(1):62–73, 1999.

[6] Hervé Delingette, Stéphane Cotin, and Nicholas Ayache. A hybrid elastic model allowing real-time cutting, deformations and force-feedback for surgery training and simulation. In *CA '99: Proceedings of the Computer Animation*, page 70, Washington, DC, USA, 1999. IEEE Computer Society.

[7] Carlos Felippa. Introduction to finite element methods. Department of Aerospace Engineering Sciences and Center for Aerospace Structures, University of Colorado, 2004.

[8] V. Ferrari, C. Cappelli, G. Megali, and A. Pietrabissa. An anatomy driven approach for generation of 3d models from multi-phase ct images. *Proceedings of the International Congress and Exhibition. IJCARS Volume 3, Supplement 1 / June*, 2008.

[9] Marc Hollenstein, Alessandro Nava, Davide Valtorta, Jess G. Snedeker, and Edoardo Mazza. Mechanical characterization of the liver capsule and parenchyma. In *ISBMS*, pages 150–158, 2006.

[10] Ryo Kikuuwe, Hiroaki Tabuchi, and Motoji Yamamoto. An edge-based computationally efficient formulation of saint venant-kirchhoff tetrahedral finite elements. *ACM Trans. Graph.*, 28(1):1–13, 2009.

[11] Man Liu and D. G. Gorman. Formulation of rayleigh damping and its extensions. *Computers & Structures*, 57(2):277–285, 1995.

[12] Bryn Lloyd, Gbor Szkely, and Matthias Harders. Identification of spring parameters for deformable object simulation. *IEEE Transactions on Visualization and Computer Graphics*, 13:1081–1094, 2007.

[13] Bin Luo, Ronghua Yang, Peng Ying, M. Awad, M. Choti, and R. Taylor. Elasticity and echogenicity analysis of agarose phantoms mimicking liver tumors. In *Bioengineering Conference, 2006. Proceedings of the IEEE 32nd Annual Northeast*, pages 81–82, apr 2006.

[14] Andrea Moglia, Giuseppe Turini, Vincenzo Ferrari, Mauro Ferrari, and Franco Mosca. Patient specific surgical simulator for the evaluation of the movability of bimanual robotic arms. *Studies in Health Technology and Informatics*, 163:379–385, 2011.

[15] Neil Molino, Robert Bridson, Joseph Teran, and Ronald Fedkiw. A crystalline, red green strategy for meshing highly deformable objects with tetrahedra. In *In 12th Int. Meshing Roundtable*, pages 103–114, 2003.

[16] Wouter Mollemans, Filip Schutyser, Johan Van Cleynenbreugel, and Paul Suetens. Tetrahedral mass spring model for fast soft tissue deformation. In *IS4TM'03: Proceedings of the 2003 international conference on Surgery simulation and soft tissue modeling*, pages 145–154, Berlin, Heidelberg, 2003. Springer-Verlag.

[17] A. Nava, E. Mazza, M. Furrer, P. Villiger, and W.H. Reinhart. In vivo mechanical characterization of human liver. *Medical Image Analysis*, 12(2):203–216, 2008.

[18] Chris H. Rycroft. Voro++: A three-dimensional voronoi cell library in c++. *Chaos: An Interdisciplinary Journal of Nonlinear Science*, 19(4):041111, 2009.

[19] G. San Vicente, C. Buchart, D. Borro, and J. Celigeta. Maxillo-facial surgery simulation using a mass-spring model derived from continuum and the scaled displacement method. *International Journal of Computer Assisted Radiology and Surgery*, 4:89–98, 2009. 10.1007/s11548-008-0271-0.

[20] J Schoberl. Netgen - an advancing front 2d/3d mesh generator based on abstract rules. *Computing and Visualization in Science*, 1(1):41–52, 1997.

[21] J. F. Semblat. Rheological interpretation of rayleigh damping. *Journal of Sound and Vibration*, 206(5):741–744, 1997.

[22] Baoxiang Shan, Assimina A. Pelegri, Caroline Maleke, and Elisa E. Konofagou. A mechanical model to compute elastic modulus of tissues for harmonic motion imaging. *Journal of Biomechanics*, 41(10):2150–2158, 2008.

[23] Allen Van Gelder. Approximate simulation of elastic membranes by triangulated spring meshes. *J. Graph. Tools*, 3(2):21–42, 1998.

[24] Davide Zerbato, Stefano Galvan, and Paolo Fiorini. Calibration of mass spring models for organ simulations. In *IROS*, pages 370–375, 2007.